Inorg. Chem. **2005**, *44*, 3818–3826

Definitive Assignments of the Visible–Near-IR Bands of Porphyrin-Naphthalocyanine Rare-Earth Sandwich Double- and Triple-Decker Compounds by Magnetic Circular Dichroism Spectroscopy

Atsuya Muranaka,*,‖ Yotaro Matsumoto,‡ Masanobu Uchiyama,‡ Jianzhuang Jiang,§ Yongzhong Bian,§ Arnout Ceulemans,*,‖ and Nagao Kobayashi*,†

Department of Chemistry, Graduate School of Science, Tohoku University, Sendai, 980-8578, Japan, Graduate School of Pharmaceutical Sciences, The University of Tokyo, Tokyo, 113-0033, Japan, and PRESTO, Japan Science and Technology Agency (JST), Japan, Department of Chemistry, Shandong University, Jinan, 250100, China, and Division of Quantum Chemistry, Katholieke Universiteit Leuven, Celestijnenlaan, 200F, B-3001, Leuven, Belgium

Received February 14, 2005

A series of heteroleptic rare-earth sandwich complexes [M(Nc)(OEP)] (M = La, Nd, Eu, Dy, and Lu; Nc = 2,3-naphthalocyaninate; OEP = octaethylporphyrinate) have been investigated by electronic absorption and magnetic circular dichroism (MCD) spectroscopy. The electronic absorption spectra of the neutral forms showed two characteristic transitions (bands I and II) in the near-IR region, both of which were systematically shifted depending on the size of their central metal. In the MCD spectra, a relatively intense Faraday *A* term and a significantly weak Faraday *B* term have been observed corresponding to bands II and I, respectively. The spectral features were successfully interpreted using a simple MO model by considering the relevant interactions of Gouterman's four orbitals of the constituent chromophores. The model succeeded in assigning the MCD spectra of the related compounds, the oxidized and reduced forms of the dimer ($[M(Nc)(OEP)]^+$ and $[M(Nc)(OEP)]^-$), and neutral forms of the triple-decker compounds ($M_2(Nc)(OEP)_2$, M = Nd, Eu). DFT calculations of the dimers supported the validity of this model.

Introduction

Porphyrins and related macrocycles such as phthalocyanines and naphthalocyanines are important classes of pigments because of their actual or potential applications in various fields.[1] In particular, sandwich-type oligomers consisting of these chromophores have attracted considerable interest, not only with respect to fundamental aspects but also in areas of material science, such as electrochromic displays, near-IR dyes, and organic conductors, since they exhibit remarkable spectral features that cannot be found in monomeric porphyrinoids.[2] Recently, we have reported the synthesis and characterization of rare-earth sandwich compounds with mixed 2,3-naphthalocyaninato (Nc) and octaethylporphyrinato (OEP) ligands.[3] It was found that the electronic absorption spectra of the sandwich dimers [M(Nc)(OEP)] vary systematically depending on the size of the central metal. In this study, the magnetic circular dichroism

* Authors to whom correspondence should be addressed. E-mail: nagaok@mail.tains.tohoku.ac.jp (N.K.); Arnout.Ceulemans@chem.kuleuven.ac.be (A.C.).
† Tohoku University.
‡ The University of Tokyo and PRESTO.
§ Shandong University.
‖ Katholieke Universiteit, Leuven.

(1) (a) Mckeown, N. B. *Phthalocyanine Materials*; Cambridge University Press: Cambridge, U.K., 1998. (b) *Phthalocyanines-Chemistry and Functions*; Shirai, H., Kobayashi, N., Eds.; I. P. C.: Tokyo, 1997. (c) *The Porphyrin Handbook*; Kadish, K. M., Smith, K. M., Guilard, R., Eds.; Academic Press: New York, 2000; Vols. 1−20.

(2) (a) Buchler, J. W.; Ng. D. K. P. In *The Porphyrin Handbook*, Vol. 3; Kadish, K. M., Smith, K. M., Guilard, S. M., Eds.; Academic Press: New York, 2000; Chapter 20, pp 245−294. (b)Wei, L.; Padmaja, L.; Youngblood, W. J.; Lysenko, A. B.; Lindsey, J. S.; Bocian, D. F. *J. Org. Chem.* **2004**, *69*, 1461−1469. (c) Zhang, H.; Wang, R.; Zhu, P.; Lai, Z.; Han, J.; Choi, C.-F.; Ng, D. K.; Chi, X.; Ma, C.; Jiang, J. *Inorg. Chem.* **2004**, *43*, 4740−4742. (d) Jiang, J.; Liu, W.; Arnold, D. P. *J. Porphyrins Phthalocyanines* **2003**, *7*, 459−473. (e) Furuya, F.; Ishii, K.; Kobayashi, N. *J. Am. Chem. Soc.* **2002**, *124*, 12652−12653. (f) Kobayashi, N. *Coord. Chem. Rev.* **2002**, *227*, 129−152. (g) Jiang, J.; Kasuga, K.; Arnold, D. P. In *Supramolecular Photosensitive and Electro-active Materials*; Nalwa, H. S., Ed.; Academic Press: New York, 2001; pp 113−210. (h) Takeuchi, M.; Imada, T.; Shinkai, S. *Angew. Chem., Int. Ed.* **1998**, *37*, 2096−2099. (i) Ng, D. K. P.; Jiang, J. *Chem. Soc. Rev.* **1997**, *26*, 433−442. (j) Kadish, K. M.; Moninot, G.; Hu, Y.; Dubois, D.; Ibnlfassi, A.; Barbe, J.-M.; Guilard, R. *J. Am. Chem. Soc.* **1993**, *115*, 8153−8166.

10.1021/ic0502325 CCC: $30.25
Published on Web 04/26/2005

(MCD) spectra of these complexes are recorded in the range of 300−2000 nm, to gain a better understanding of the characteristic spectral features. The results are successfully explained on the basis of a simple molecular orbital (MO) model by considering the relevant interactions of Gouterman's four orbitals[4] of the constituent chromophores. The interpretation of the electronic absorption spectra of even homoleptic rare-earth sandwich complexes of phthalocyanines has not necessarily been consistent among researchers in the past.[5] However, as shown in this paper, by comparing the spectra of a series of heteroleptic naphthalocyaninato and porphyrinato sandwich complexes, the assignments of the visible to near-IR absorption bands of these sandwich complexes become unambiguous.

MCD spectroscopy is a powerful technique to complement electronic absorption spectra, since MCD spectra are more sensitive than normal absorption spectra to structural modifications that directly affect the electronic energy levels of porphyrinoids.[6] The MCD signal arises from the same transitions as those seen in the UV−vis absorption spectrum, but the selection rules are different since the intensity mechanism depends on the magnetic dipole moment in addition to the electric dipole moment, which normally determines the UV−vis absorption intensity. There are two terms (Faraday *A* and *B* terms) that can contribute to MCD spectra of porphyrinoids with orbitally nondegenerate ground states. The Faraday *A* term arises for transitions involving degenerate final states and will occur in molecules with at least a threefold symmetry axis such as D_{4h} metalloporphyrins. The shape of the *A* term corresponds to a first derivative of an absorption line.[7] In contrast, the Faraday *B* term arises from magnetically induced mixing of nondegenerate states, and the shape is similar to that of the absorption band.[8] The appearance of each MCD signal is illustrated in Figure 1. In the case of a molecule with degenerate ground states, the Faraday *C* term is observed. The intensity of the *C* term is inversely proportional to temperature, and the shape is normally Gaussian type.[9]

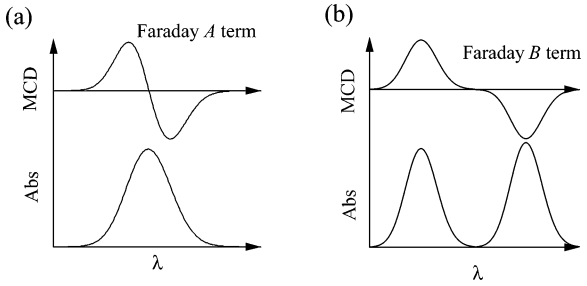

Figure 1. Illustration of typical MCD signals. (a) Faraday *A* term. (b) Faraday *B* term.

Chart 1. (a) Compounds in this study. (b) Schematic Geometry of the π Skeletons of Sandwich Heterodimer (Staggered Conformation with Twist Angle $\theta = 45°$)

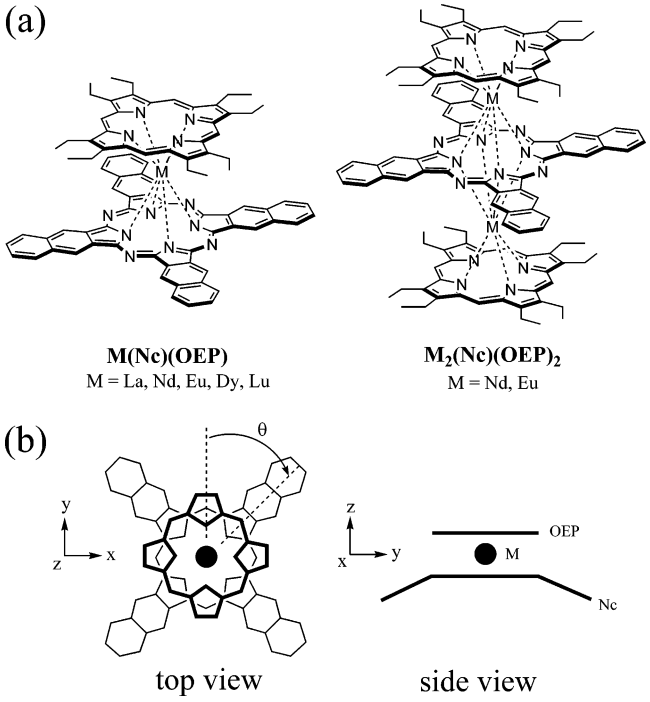

Chart 1 shows the structures of the sandwich complexes of the present study. The neutral form of the dimer is a radical complex in which the hole or unpaired electron is delocalized over the two rings. This has been confirmed by EPR, NMR, and IR spectroscopy.[3] Since the interplanar distance of this type of complexes (2.65−3.06 Å) was closer than their van der Waals distance (3.4 Å),[3] electron exchange interactions play an important role in the electronic structures. In such a case, an MO model is more appropriate than an exciton model to understand the spectroscopic properties. Indeed, Ishikawa et al. successfully interpreted the spectral features of some homoleptic sandwich phthalocyanine complexes by calculating the MOs.[10] The previous single-crystal X-ray analyses have revealed that the complexes (M(Nc)(OEP),

(3) (a) Jiang, J.; Bian, Y.; Furuya, F.; Liu, W.; Choi, M. T. M.; Kobayashi, N.; Li, H.-W.; Yang, Q.; Mak, T. C. W.; Ng, D. K. P. *Chem. Eur. J.* **2001**, *7*, 5059−5069. (b) Furuya, F.; Kobayashi, N.; Bian, Y. Z.; Jiang, J. Z. *Chem. Lett.* **2001**, *9*, 944−945. (c) Bian, Y.; Wang, D.; Wang, R.; Weng, L.; Dou, J.; Zhao, D.; Ng, D. K. P.; Jiang, J. *New. J. Chem.* **2003**, *27*, 844−849. (d) Bao, M.; Bian, Y. Z.; Rintoul, L.; Wang, R. M.; Arnold, D. P.; Ma, C. Q.; Jiang, J. Z. *Vib. Spectrosc.***2004**, *34*, 283−291.

(4) (a) Gourterman, M. In *The Porphyrins, Volume III, Physical Chemistry, Part A*; Dolphin, D., Ed.; Academic Press: New York, 1978; pp 1−156. (b) Gouterman, M. J. *Chem. Phys.* **1959**, *30*, 1139−1161. (c) Gouterman, M. J. *Mol. Spectrosc.* **1961**, *6*, 138−163. (d) Ceulemans, A.; Oldenhof, W.; Görller-Walrand, C.; Vanquickenborne, L. G. *J. Am. Chem. Soc.* **1986**, *108*, 1155−1163.

(5) (a) Konami, H.; Hatano, M.; Tajiri, A. *Chem. Phys. Lett.* **1990**, *166*, 605−608. (b) Markovitsi, D.; Tran-Thi, T.-H.; Even, R.; Simon, J. *Chem. Phys. Lett.* **1987**, *137*, 107−112.

(6) (a) Rodger, A.; Nordén, B. *Circular Dichroism and Linear Dichroism*; Oxford University Press: Oxford, U.K., 1997. (b) Michl, J. *J. Am. Chem. Soc.* **1978**, *100*, 6801−6811. (c) Michl, J. *J. Am. Chem. Soc.* **1978**, *100*, 6812−6818.

(7) (a) Miwa, H.; Ishii, K.; Kobayashi, N. *Chem. Eur. J.* **2004**, *10*, 4422−4435. (b) Ishii, K.; Kobayashi, N.; Matsuo, T.; Tanaka, M.; Sekiguchi, A. *J. Am. Chem. Soc.* **2001**, *123*, 5356−5357. (c) Kobayashi, N.; Mack, J.; Ishii, K.; Stillman, M. J. *Inorg. Chem.* **2002**, *41*, 5350−5363.

(8) (a) Muranaka, A.; Okuda, M.; Kobayashi, N.; Somers, K.; Ceulemans, A. *J. Am. Chem. Soc.* **2004**, *126*, 4596−4604. (b) Borovkov, V. V.; Fujii, I.; Muranaka, A.; Hembury, G. A.; Tanaka, T.; Ceulemans, A.; Kobayashi, N.; Inoue, Y. *Angew. Chem., Int. Ed.* **2004**, *43*, 5481−5485. (c) Muranaka, A.; Yokoyama, M.; Matsumoto, Y.; Uchiyama M.; Tsuda, A.; Osuka, A.; Kobayashi, N. *ChemPhysChem*, **2005**, *6*, 171−179. (d) Fukuda, T.; Makarova, E. A.; Luk'yanets, E. A.; Kobayashi, N. *Chem. Eur. J.* **2004**, *10*, 117−133.

(9) (a) Kobayashi, N.; Koshiyama, M.; Osa, T. *Inorg. Chem.* **1985**, *24*, 2502−2508. (b) Kobayashi, N.; Nozawa, T.; Hatano, M. *Bull. Chem. Soc. Jpn.* **1981**, *54*, 919−920. (c) Kobayashi, N.; Osa, T. *Chem. Pharm. Bull.* **1989**, *37*, 3105−3107.

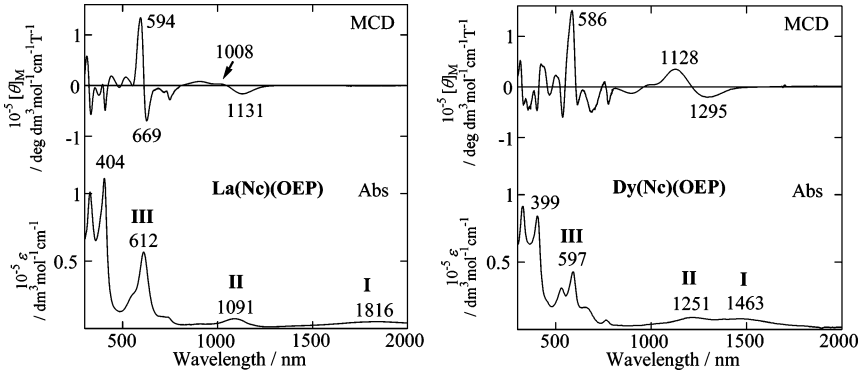

Figure 2. Electronic absorption and MCD spectra of La(Nc)(OEP) (left) and Dy(Nc)(OEP) (right) recorded in $CHCl_3$ at room temperature.

Table 1. Electronic Absorption and MCD Data for the Neutral Form of [M(Nc)(OEP)] in the Near-IR Region in $CHCl_3$ at Room Temperature

central metal (ionic radius)	assignment	abs λ (nm)	$10^{-4}\,\epsilon$ (dm^3 mol^{-1} cm^{-1})	MCD λ (nm)	$10^{-3}[\theta]_M$ (deg dm^3 mol^{-1} cm^{-1} T^{-1})
La	I	1816	0.29	1823	−0.6
(116 pm)	II	1091	0.42	1131, 1008	−16.4, 3.0
Nd	I	1642	0.58	1658	−1.5
(110.9 pm)	II	1157	0.65	1196, 1060	−28.4, 5.0
Eu	I	1542	0.58	1591	−1.1
(106.6 pm)	II	1196	0.71	1244, 1102	−22.0, 3.5
Dy	I	1463	0.72	1463(sh)	−2.0
(102.7 pm)	II	1251	0.79	1295, 1128	−20.5, 34.9
Lu	I (and II)	1336	0.78	1323, 1038	−10.2, 4.1
(97.7 pm)					

M = La, Pr, Nd, Sm, Eu, Gd, Tb, Dy, Ho, Er, Yb, Lu, Y) adopt a conformation in which the two chromophoric units are almost fully staggered with respect to the pyrrole nitrogen atoms, regardless of the size of the central metal (Chart 1b).[3] Thus, the twist angle θ, defined as the rotation angle of one ring away from the eclipsed conformation of the two rings, is close to 45° (approximately C_{4v} symmetry) in the crystal structure. This is in contrast to the crystal structure of a series of bis(phthalocyaninato) lanthanide(III) complexes, in which the twist angle increases with decreasing size of the central metal.[11] A series of the OEP−Nc dimers, therefore, appears to be an ideal system for analyzing their systematic spectral changes on the basis of MO models: conformational flexibilities, which sometimes cause unreliable MO analyses, are negligible in this system.

Experimental Section

Measurements. Synthesis and characterization of the compounds in this study have been reported previously.[3a] Electronic absorption spectra were recorded using a Hitachi U-3410 spectrophotometer in a 1-cm quartz cell in chloroform at room temperature. MCD spectra were recorded in the range of 300−900 nm with a JASCO J-725 spectrodichrometer equipped with a JASCO electromagnet which produces parallel and antiparallel magnetic fields of 1.09 T, and in the near-IR region (800−2000 nm) with a JASCO J-730 spectrodichrometer equipped with a JASCO electromagnet which produces magnetic fields of 1.5 T. The MCD spectra were combined in the region where there are no intense absorption bands. The magnitude of the MCD signal is expressed in terms of molar ellipticity per tesla ($[\theta]_M$/deg dm^3 mol^{-1} cm^{-1} T^{-1}). Typical MCD scanning conditions for the near-IR region (800−2000 nm) were scanning rate = 50 nm per min, bandwidth = 10 nm, response time = 4 s, accumulations = 2 scans, sensitivity = 50 mdeg, sample concentration (for La(OEP)(Nc)) = 2.24×10^{-4} M.

Calculations. The geometry optimizations of the sandwich dimers were calculated at the DFT/B3LYP level of theory using C_{4v} symmetry restriction as implemented in TURBOMOLE.[12] Split valence basis sets augmented with polarization functions (def-SV-(P)) were used for all calculations. Lanthanide atoms were represented by the generic La atom, with 46 electrons in the effective core and a 13s4p1d/[8s2p1d] valence shell. The neutral form was calculated within the spin unrestricted approximation, while the reduced and oxidized forms were calculated within the restricted closed-shell approximation. The molecular orbital (MO) analysis in this study is based on the Kohn−Sham molecular orbitals generated by the DFT method. The frontier orbitals were constructed by linear combinations of the constituent monomeric MOs. Analogous MO features were obtained when the sandwich dimers (Y(Nc)(OEP)) were calculated at the semiempirical ZINDO/1 level, as implemented in HyperChem.[13]

Results and Discussion

Neutral Form of M(Nc)(OEP). Spectroscopic Properties. Typical electronic absorption and MCD spectra of the

(10) (a) Ishikawa, N.; Kaizu, Y. *Chem. Phys. Lett.* **2001**, *339*, 125−132. (b) Ishikawa, N.; Ohno, O.; Kaizu, Y. *J. Phys. Chem.* **1993**, *97*, 1004−1010. (c) Ishikawa, N.; Ohno, O.; Kaizu, Y.; Kobayashi, H. *J. Phys. Chem.* **1992**, *96*, 8832−8839. (d) Ishikawa, N.; Ohno, O.; Kaizu, Y. *Chem. Phys. Lett.* **1991**, *180*, 51−56.

(11) Koike, N.; Uekusa, H.; Ohashi, Y.; Harnoode, C.; Kitamura, F.; Ohsaka, T.; Tokuda, K. *Inorg. Chem.* **1996**, 35, 5798−5804.

(12) Ahlrichs, R.; Bär, M.; Baron, H.-P.; Bauernschmitt, R.; Böcker, S.; Ehrig, M.; Eichkorn, K.; Elliot, S.; Haase, F.; Häser, M. Horn, H.; Huber, C.; Huniar, U.; Kattannek, M.; Kölmel, C.; Kollwitz, M.; Ochsenfeld, C.; Öhm, H.; Schäfer, A.; Schneider, U.; Treutler, O.; von Arnim, M.; Weigend, F.; Weis, P.; Weiss, H. *TURBOMOLE*, version 5.6; Quantum Chemistry Group, University of Karlsruhe: Karlsruhe, Germany, 2002.

(13) *HyperChem 5.01 Windows Molecular Modeling System*; HyperCube, Inc.: Canada, 1996.

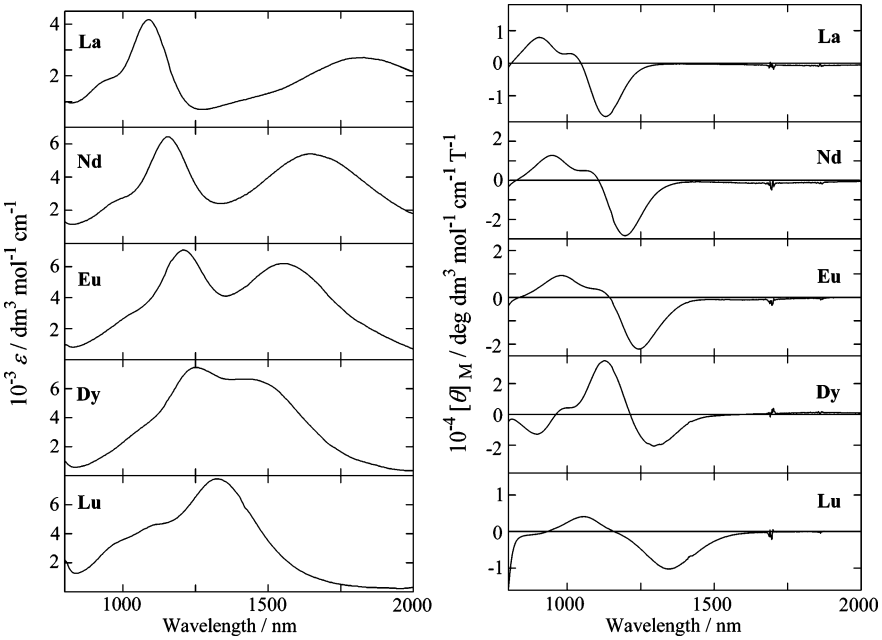

Figure 3. Dependence of the central atom of the sandwich dimer (M(Nc)(OEP)) on the near-IR absorption (left) and MCD (right) spectra. The MCD signals at ca. 1650 and 1800 nm are due to C−H vibration of the solvent ($CHCl_3$).

neutral form of sandwich dimers (La(Nc)(OEP) and Dy(Nc)-(OEP)) in $CHCl_3$ are shown in Figure 2, with the values of the spectra tabulated in Table 1, together with assignments of the bands to electronic transitions. As we previously reported, the peak positions of the absorption bands depend strongly on the ionic radius of the central metal. Bands I and II undergo red- and blue-shifts, respectively, as the ionic radius increases, while the spectral shift of Band III is relatively small. It was found that the MCD signal corresponding to Band I is an extremely weak absorption-type signal, which can be attributed to a Faraday *B* term. In contrast, the MCD signals of Band II were assigned to a Faraday *A* term. The signal pattern of the Dy dimer has a typical first derivative shape, while that of the La dimer is less resolved. This may arise from overlap with a vibronic sideband. This kind of Faraday *A* term was observed for some phthalocyanine derivatives reported previously.[13] The most intense MCD signals, which appear to be a first derivative of the absorption band, were observed at about 600 nm (B and III). This type of intense signal should be correlated to the Q-band nature with a large magnetic dipole moment. The intense absorption bands with weaker MCD signals seen at ca. 400 nm are attributable to the Soret bands.

Figure 3 shows the dependence of the near-IR spectra on the size of the central rare-earth metal. It is clearly seen that the excitation energies corresponding to Bands I and II are systematically shifted and that the MCD appearances (sign and intensity) are essentially similar throughout the series. Assuming a systematic change, Bands I and II of the Lu complex are in the same absorption envelope. The absorption shoulder seen in the higher energy region of Band II may be a vibronic band of Band II.

MO Analysis. To explain the observed spectral features of the sandwich dimers, let us first introduce the relationship between the spectroscopic properties of monomeric OEP and Nc, and Gouterman's four orbitals. A metallo OEP generally exhibits a significantly weak visible absorption band at 500−600 nm (Q-band), while a metallo Nc shows sharp, intense Q-bands beyond 750 nm because of the extended π system.[1] Figure 4 shows Gouterman's four orbitals of OEP and Nc units.[4] Both compounds have degenerate LUMO (e_g) because of D_{4h} symmetry. The coefficients of the degenerate LUMO can be arbitrarily chosen. As shown in Figure 4, coefficients of the LUMOs are chosen to be matching canonical components of the degenerate symmetry representation when the sandwich dimer is formed. It is seen from Figure 5 that the energy level of the HOMO-1 (a_{2u}) of OEP is close to that of the HOMO (a_{1u}). As a result, a significant mixing of the HOMO and HOMO-1 to LUMO (degenerate) occurs, leading to cancellation of the transition moments in the Q-bands. In contrast, the a_{2u} orbital (HOMO-1) of the Nc is strongly stabilized because of the higher electronegativity of the *meso*-nitrogen atoms, while the a_{1u} orbital (HOMO) is considerably destabilized because of antibonding interactions with the fused naphthalene rings. This causes a smaller HOMO−LUMO gap and less mixing of these transitions, resulting in an intense near-IR Q transition.

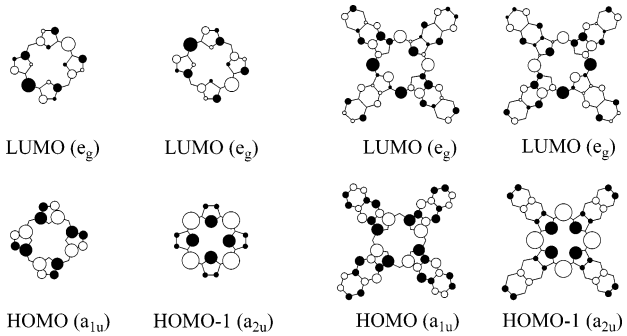

Figure 4. Gouterman's four orbitals of OEP and Nc chromophores. Peripheral ethyl groups are omitted for clarity.

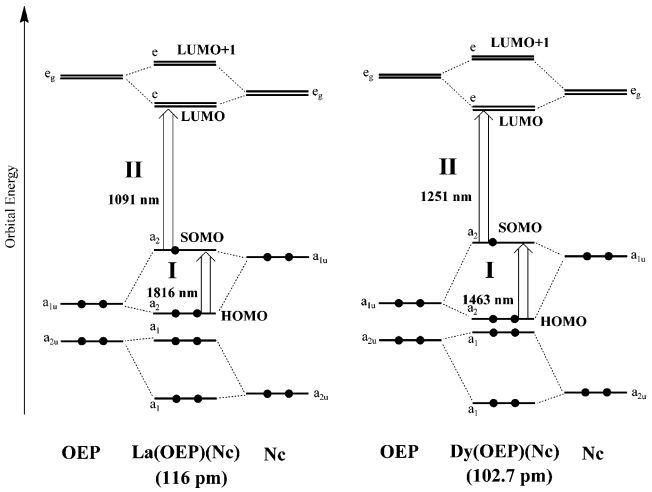

Figure 5. Schematic representation of the frontier MO energies for the C_{4v} sandwich dimer (M(OEP)(Nc)) with larger (M = La) and smaller (M = Dy) central metals. The value in parentheses indicates the size of the central metal.

An MO model comprising Gouterman's orbitals of OEP and Nc chromophores is then considered. In general, interaction with two monomeric MOs gives two new MOs, one of lower energy than the lower of the two monomeric MOs, the other of higher energy than the higher of the same two MOs. The MOs of the present dimer contain a greater contribution from the monomeric MO which is closer in energy to the new MO. Since the HOMO−LUMO gap of Nc is smaller than that of OEP,[1,15] the following features can be deduced for the frontier MOs of the OEP−Nc system: the SOMO (singly occupied molecular orbital) and LUMO (degenerate) contain a greater contribution from Nc, while the HOMO and LUMO+1 (degenerate) have a greater contribution from OEP. Consequently, the schematic MO diagrams of a dimer with a large or small central metal become as illustrated in Figure 5. Schematic illustrations of the bonding and antibonding interactions between the AOs are shown in Figure 6. First, it should be noted that there is no interaction between the a_{1u} and a_{2u} orbitals because of their different symmetry. In addition, we can assume that the pyrrole α carbon interactions ($C_\alpha-C_\alpha$) contribute mainly to the MOs of the dimer, since these moieties are the closest positions in the eclipsed conformation. This interaction is quite evident in the $a_{1u}-a_{1u}$ interaction.

On the basis of the MO models, the absorption bands I and II can be assigned to the HOMO→SOMO and SOMO→LUMO transitions, respectively. These assignments are in agreement with the observed MCD signals: the HOMO(a_2)→SOMO(a_2) transition is a nondegenerate transition that has a CT character (from OEP to Nc), which correlates with the Faraday *B* term (absorption-shape MCD signal) observed in the MCD spectra. The transition polarization is parallel to the *z*-axis (see Chart 1b). Since the transition moment between two states of a_2 symmetry has a_1 symmetry ($a_2 \times a_2 = a_1$), the transition becomes electric dipole allowed, but magnetic dipole forbidden on the basis of the group theory. The small intensity of the MCD may be essentially the result of the transfer character of the transition, which gives rise to small oscillator strength of the absorption spectrum. On the other hand, the SOMO(a_2)→LUMO(e) transition is a degenerate transition that has a $\pi-\pi^*$ transition character (Nc's Q-band character) with *x*- or *y*-axis polarization, correlating with the Faraday *A* term observed in the MCD spectra. Since the $\pi-\pi^*$ transition of porphynoids has a relatively large magnetic moment,[4] an intense MCD signal is predicted. In addition, the MCD spectral shape observed for Band II is explained as follows. Since the SOMO→LUMO transition corresponds to the promotion of one electron from the antibonding a_2 orbital to the bonding e orbital, the potential energy curve of this state, along with the inter-macrocyclic distance coordinate, is expected to be displaced to give a shorter Nc−OEP distance, relative to the ground state. This leads to a shift of the Franck−Condon intensity from the origin to higher vibronic components.[16] As a result, a significant convolution of the Franck−Condon 0−0 band and the vibronic bands occurs for Band II. The dome-shaped structure of the Nc ring may also contribute to the intensity redistribution. The weak absorption bands observed between Bands II and III (ca. 550−700 nm) may be ascribed to CT transitions such as the HOMO→LUMO (transition from OEP to Nc) and SOMO→LUMO+1 transitions (transition from Nc to OEP), judging from their optically forbidden nature.

The dependence of the size of the central metal on the absorption peak positions can be reasonably explained using the simple MO model. In the case of a larger central metal, the HOMO−SOMO energy gap is smaller than the SOMO−LUMO energy gap because of the smaller overlap between AOs corresponding to the pyrrole α-carbons. This causes the well-separated excitation energies of Bands I and II. In contrast, in the case of a smaller central metal, the HOMO−SOMO energy gap becomes comparable to the SOMO−LUMO energy gap because of the larger overlap between the monomeric MOs, so that the energy gap between Bands I and II decreases considerably. This MO model is consistent with the electrochemical properties, which showed a linear correlation between the redox potentials and the size of the central metal.[3a] Here, the first oxidation potential, which is related to the SOMO energy, decreases when the ionic radius of the central metal becomes smaller.

As mentioned earlier, relatively intense MCD signals were observed for Band III. This should be related to the Q-band character, because the orbital angular momentum for the Q transition is in general larger than the other transitions.[4] Thus, Band III can be attributed to a transition having the OEP's Q-band character (HOMO→LUMO+1).

We now comment on the MCD signs observed for Band II. According to Michl's perimeter model, the sign sequence

(14) (a) Kobayashi, N.; Miwa, H.; Nemykin, V. N. *J. Am. Chem. Soc.* **2002**, *124*, 8007−8020. (b) Kobayashi, N.; Fukuda, T. *J. Am. Chem. Soc.* **2002**, *124*, 8021−8034.

(15) Kobayashi, N.; Konami, H. In *Phthalocyanines, Properties and Applications*; Leznoff, C. C., Lever, A. B. P., Eds.; VCH Publishers: New York, 1989; Vol. 4, pp 349−404.

(16) Ricciardi, G.; Rosa, A.; Baerends, E. J.; van Gisbergen, S. A. J. *J. Am. Chem. Soc.* **2002**, *124*, 12319−12334.

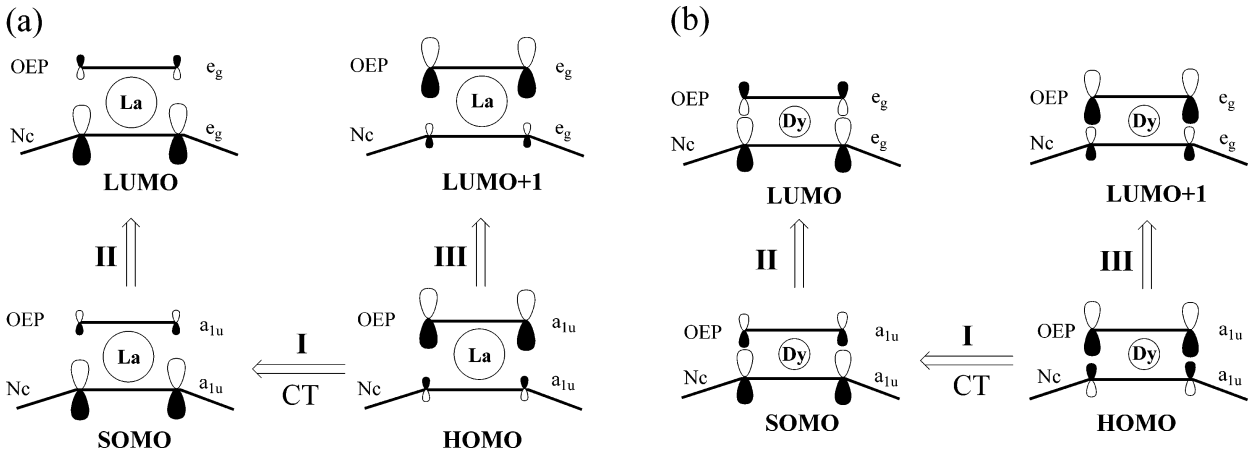

Figure 6. Schematic representation of the bonding and antibonding interactions of (a) dimer with larger metal (b) dimer with smaller metal. The size of the orbital corresponds to the coefficient of the dimer's MOs.

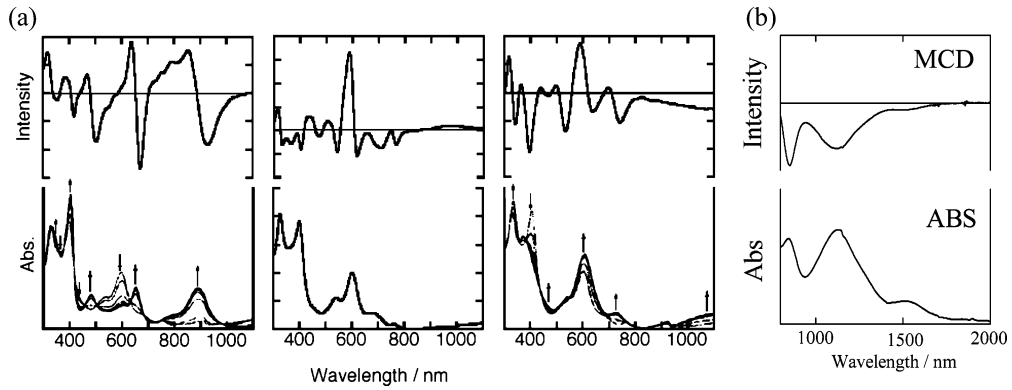

Figure 7. (a) Electronic absorption and MCD spectra of the reduced, neutral, and oxidized form of Eu(Nc)(OEP) from left to right (redrawn from ref 3b). (b) Electronic absorption and MCD spectra of $[Eu(Nc)(OEP)]^+$ in the near-IR region. The absorption at ca. 1500 nm may arise from the neutral form.

of Faraday *A* terms is predicted by assessing the orbital degeneracy of the frontier MOs.[6,17] When the LUMO and HOMO are degenerate and nondegenerate, a negative/positive first-derivative signal pattern is predicted with increasing energy. The MCD signals of high-symmetry porphyrin and related compounds have been in agreement with theory. The negative/positive MCD signs for Band II of the present dimers indicate that the degeneracy of the LUMO remains unchanged.

Oxidized and Reduced Forms of M(Nc)(OEP). The neutral form of the dimer is reported to be easily oxidized or reduced by chemical or electrochemical methods.[3a,3b] The spectroscopic properties of the dimer vary dramatically, depending on the changes in molecular charge. For example, the spectra of the neutral, oxidized, and reduced forms of Eu(Nc)(OEP) are shown in Figure 7. Two near-IR absorption bands observed at 1196 nm (band II) and 1542 nm (band I) for the neutral form disappeared in both the reduced and oxidized forms. A new absorption band appeared at 900 nm for the reduced form, while a new absorption band appeared at 1100 nm for the oxidized form. The MCD spectra clearly indicate a first-derivative pattern (Faraday *A* term) for the absorption band at 900 nm of $[Eu(Nc)(OEP)]^-$, while the absorption shape (Faraday *B* term) for the absorption at 1100 nm of $[Eu(Nc)(OEP)]^+$, thus indicating transitions to degenerate and nondegenerate states, respectively. The absorption and MCD spectral patterns of the other metal complexes are essentially identical to the Eu complexes, although the peak positions of the reduced and oxidized forms are also systematically changed, depending on the size of the central metal.

The simple MO model discussed in the previous section can account for the spectral changes of the reduced and oxidized systems. The oxidation process corresponds to the removal of one electron from the SOMO of the neutral form, while the reduction process corresponds to addition of one electron to the SOMO. The change in the number of electrons on the antibonding MO results in a geometrical change in the dimer: in the case of the reduced dimer, the antibonding orbital (i.e., the SOMO of the neutral species) is filled with two electrons to become the HOMO, so that the Nc−OEP distance increases to some extent because of electrostatic repulsion between the two rings. This results in a smaller energy gap between the bonding (for example, HOMO-1) and antibonding (for example, HOMO) MOs, and as a result, the HOMO (Nc π)→LUMO (Nc π*) transition (corresponding to the SOMO→LUMO transition of the neutral form) shifts to the blue. In contrast, an electron on the antibonding occupied orbital (i.e., SOMO of the neutral species) is removed in the case of the oxidized form, leading to a smaller Nc−OEP distance because of the absence of the repulsion.

(17) Keegan, J. D.; Stolzenberg, A. M.; Lu, Y.-C.; Linder, R. E.; Barth, G.; Moscowitz, A.; Bunnenberg, E.; Djerassi, C. *J. Am. Chem. Soc.* **1982**, *104*, 4305−4317.

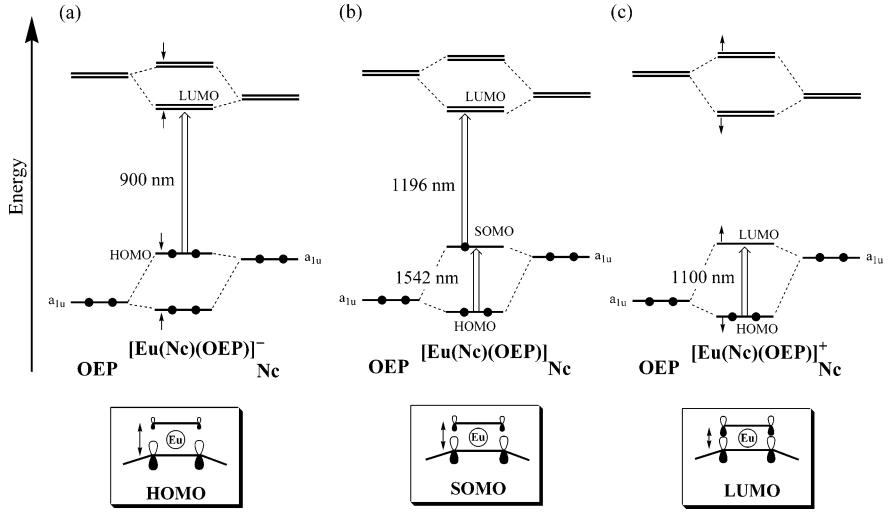

Figure 8. Schematic representation of the relative MO energy of M(Nc)(OEP). (a) The reduced form, (b) the neutral form, and (c) the oxidized form.

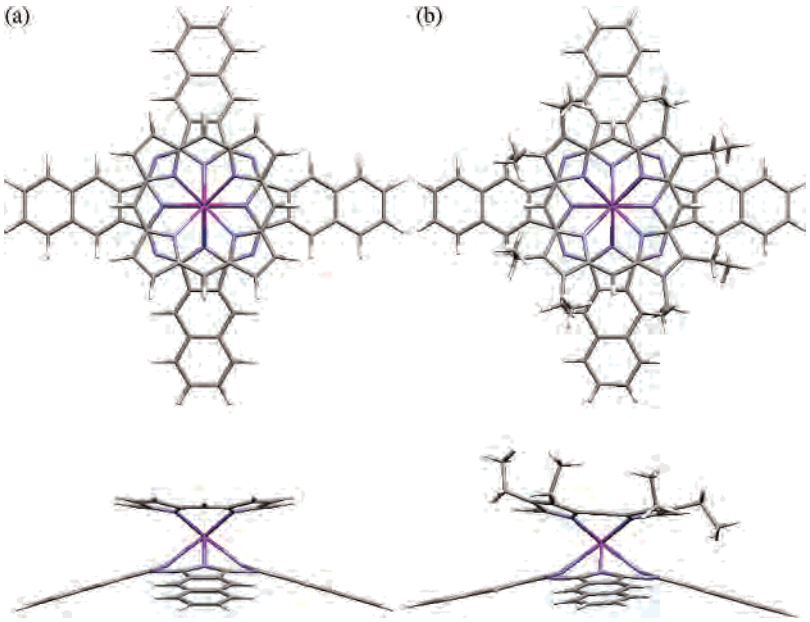

Figure 9. Top and side view of the molecular structure of Y(Nc)(OEP). (a) Optimized structure (B3LYP/def-SV(P)). (b) Crystal structure.[3a]

This results in the observation of a blue-shift of the HOMO (OEP π)→LUMO (Nc π) transition (corresponding to the HOMO→SOMO transition of the neutral form). The changes in the simple MO levels are summarized in Figure 8.

DFT Calculations. To confirm the validity of our simple MO models, geometry optimizations of the neutral, reduced, and oxidized dimers ([M(Nc)(OEP)], [M(Nc)(OEP)]$^-$, [M(Nc)-(OEP)]$^+$, M = La, Y) were carried out at the DFT/B3LYP level of theory.[12] The peripheral ethyl groups were omitted and replaced with hydrogen, and the C_{4v} symmetry restriction was used. As shown in Figure 9, the converged structure of Y(Nc)(OEP) appears to be similar to the crystal structure previously reported:[3] (1) the metal center lies closer to the N_4 plane of OEP because of the larger cavity of the OEP ring: the cavity sizes, defined as the distance between the trans pyrrole nitrogen atoms, are 4.189 Å (OEP) and 4.032 Å (Nc). (2) The Nc ring is significantly domed. Selected average bond lengths and bond angles of the Y(Nc)(OEP) system are listed in Table 2. The calculated geometrical parameters are in fairly good agreement with those of the crystal structure, although the DFT calculation seems to overestimate the distance between the central metal and

Table 2. Selected Bond Lengths (Å) and Bond Angles (deg) of the B3LYP Optimized Structure of Y(Nc)(OEP)[a]

	DFT structure (crystal structure)	
parameter[b]	OEP	Nc
$Y-N_p$	2.453 (2.407)	2.525 (2.456)
N_p-C_α	1.369 (1.370)	1.366 (1.362)
$C_\alpha-C_\beta$	1.454 (1.454)	1.474 (1.460)
$C_\beta-C_\beta$	1.366 (1.353)	1.422 (1.407)
$C_\alpha-C_m$ (N_m)	1.404 (1.384)	1.326 (1.335)
$C_\alpha-N_p-C_\alpha$	106.8 (106.1)	108.6 (107.3)
$N_p-C_\alpha-C_\beta$	109.9 (110.2)	109.9 (110.5)
$C_\alpha-C_\beta-C_\beta$	106.7 (106.7)	105.7 (105.7)
$C_\alpha-C_m(N_m)-C_\alpha$	127.3 (128.5)	124.4 (122.3)
$N_p-C_\alpha-C_m$ (N_m)	125.6 (124.6)	128.3 (128.4)

[a] The number in parenthesis indicates the averaged value calculated from the crystal structure (ref 3). [b] The C_α, C_β, and C_m atoms correspond to the pyrrole α, β, and meso carbons, respectively. N_p and N_m indicate the pyrrole and meso nitrogens.

Table 3. Calculated Distance (Å) between the Nearest Pyrrole α Carbon Atoms ($D_{\alpha\alpha}$) for the Neutral, Oxidized, and Reduced Forms of the Sandwich Dimers (M(Nc)(OEP))

central metal (ionic radius)	oxidized form	neutral form[a]	reduced form
La (116 pm)	3.634	3.677 (3.490)	3.699
Y (101.9 pm)	3.249	3.294 (3.167)	3.343

[a] The value in parentheses indicates the corresponding distance calculated from the crystal structure (ref 3).

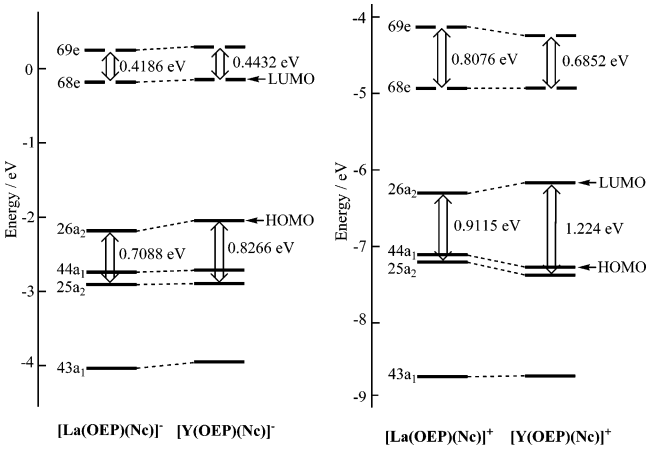

Figure 10. Selected energy level scheme for the reduced forms (left) and oxidized forms (right) of La(Nc)(OEP) and Y(Nc)(OEP) obtained from DFT/B3LYP/def-SV(P).

pyrrole nitrogen (Y−N_p) by ca. 0.05 Å (for OEP) and 0.07 Å (for Nc). This indicates that the peripheral ethyl substituent does not significantly affect the geometry of the sandwich complexes. The direction of the ethyl groups observed in the crystal structure may arise from the effect of crystal packing. Table 3 shows the distance between the nearest pyrrole α carbon atoms of the OEP and Nc rings ($D_{\alpha\alpha}$). This parameter would be directly related to the interaction between AOs on the pyrrole α carbon (C_α−C_α). According to Table 3, the value of $D_{\alpha\alpha}$ decreases in the order of reduced, neutral, and oxidized forms, so that the validity of the proposed MO model is verified.

The calculated MO energy levels are given in Figure 10. The calculated MO energy diagrams are essentially identical to those anticipated conceptionally: (1) the MOs of the sandwich dimer consist of linear combinations of the constituent monomeric MOs. (2) As the central metal becomes smaller, the bonding and antibonding energy splitting increases. Although the calculation shows that the energy of the bonding $25a_2$ orbital is lower than that of antibonding $44a_1$ orbital, the lowest optically allowed transition would still be the one between the a_2 orbitals, irrespective of the order of these two orbitals as indicated in Figure 5. This comes from the fact that the $a_1 \rightarrow a_2$ jump is symmetry forbidden ($a_1 \times a_2 = a_2$). In addition, the effect of the peripheral ethyl groups may cause the destabilization of a_{1u} orbital of a monomeric porphyrin skeleton with D_{4h} symmetry.

Neutral Form of the Sandwich Trimers, $M_2(Nc)(OEP)_2$. The above simple MO model for heteroleptic dimers can be applied to heteroleptic triple-decker systems that we have recently succeeded in preparing.[3] To date, only one crystal structure ($Nd_2(Nc)(OEP)_2$) is available.[3a] According to the crystal structure, each OEP ring is not in an ideal staggered conformation with a twist angle of ca. 45°, but adopts a conformation with a twist angle of ca. 30°. However, in this work, we assume that the geometry of the triple-decker is a fully staggered conformation with D_{4h} symmetry in solution. The electronic absorption and MCD spectra of the triple-deckers ($M_2(Nc)(OEP)_2$, M = Nd, Eu) are given in Figure 11. The lowest three absorption bands are labeled as Bands I, II, and III. All the MCD signals corresponding to Bands I, II, and III can be attributed to Faraday *A* terms because of their first derivative type shapes. As the metal size decreases, the absorption peak of Band I shifts considerably to longer wavelength, while that of Bands II and III almost do not vary (see Table 4). There is no absorption band attributable to a CT band from one chromophore to the other chromophore, unlike Band I of the sandwich dimers.

Figure 12 indicates a schematic MO energy diagram for the triple-decker system. Note that the neutral form of the trimer is not a radical complex, in contrast to the heteroleptic dimeric M(Nc)(OEP) system. The HOMO of the trimer arrises from the antibonding interaction of the a_{1u} orbitals of the three π orbitals, and the Nc ring has the largest MO coefficients. In contrast to the HOMO, the Nc plane becomes a node in the case of HOMO-1, so that the interaction energy is considered to be small. The HOMO-2 should be composed primarily of OEP orbitals and thus stabilized because of the bonding interaction of the three chromophores. Similar MO interactions are present on the unoccupied MOs. This model predicts that the HOMO−LUMO energy splitting decreases with decreasing size of the central metal. The fact that

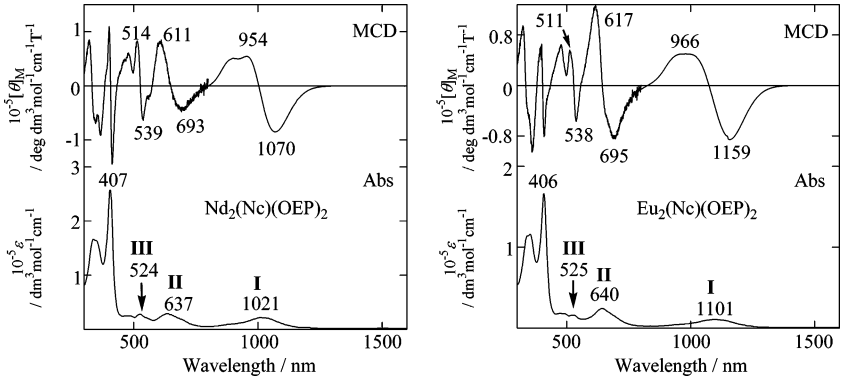

Figure 11. Electronic absorption and MCD spectra of $M_2(Nc)(OEP)_2$ (M = Nd, Eu) recorded in $CHCl_3$ at room temperature.

Table 4. Electronic Absorption and MCD Data for the Neutral Form of $[M_2(Nc)(OEP)_2]$ in $CHCl_3$

central metal (ionic radius)	assignment	abs λ (nm)	$10^{-4}\,\epsilon$ (dm^3 mol^{-1} cm^{-1})	MCD λ (nm)	$10^{-4}\,[\theta]_M$ (deg dm^3 mol^{-1} cm^{-1} T^{-1})
Nd	I	1021	2.10	1070, 954	−8.52, 5.43
(110.9 pm)	II	637	2.85	693, 611	−4.50, 7.87
	III	524	2.78	539, 514	−6.09, 8.28
Eu	I	1101	1.74	1159, 966	−2.56, 5.18
(106.6 pm)	II	640	2.42	695, 617	−3.94, 7.25
	III	525	1.61	538, 511	−6.36, 8.08

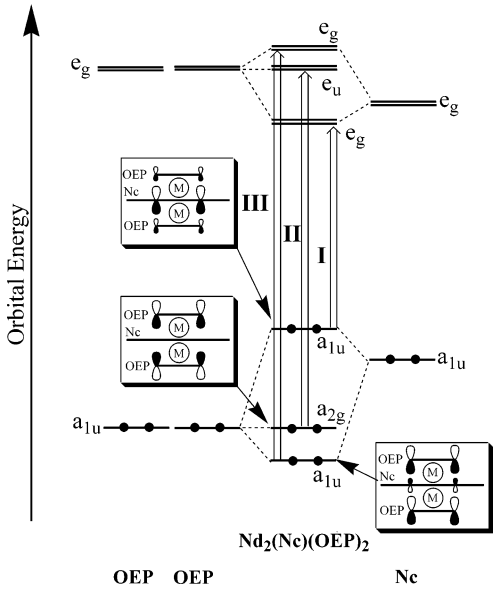

Figure 12. Schematic representation of the frontier MO energy levels of the D_{4h} triple-decker, $M_2(Nc)(OEP)_2$. Simple MO models are drawn for the three occupied MOs.

$Eu(Nc)(OEP)_2$ ($E_{1/2}$ = 0.184 V (vs SCE)) undergoes oxidation more readily than $Nd(Nc)(OEP)_2$ ($E_{1/2}$ = 0.300 V (vs SCE)) strongly indicates that our present view is rational.[3a] According to the simple MO model, band I is attributed to a HOMO−LUMO transition which possesses the Q-band character of the Nc. From the peak positions, Bands II and III are assigned to a transition from HOMO-1 to LUMO+1 and a transition from HOMO-2 to LUMO+2, respectively (Figure 12).

Conclusions

The present study has demonstrated a readily accessible and intuitive MO model to rationalize the main features of the electronic structures of the naphthalocyanine-octaethylporphyrin (OEP) rare-earth sandwich complexes (M(Nc)(OEP), M = La, Nd, Eu, Dy, and Lu). To comprehensively understand the excited states, the MCD spectra of the dimer have been measured up to 2000 nm. By considering the observed MCD signals and the MO structure of the dimer, the two lowest near-IR absorption bands (Bands I and II) of the neutral form of M(Nc)(OEP) were assigned to the HOMO→SOMO and SOMO→LUMO transitions, respectively. The MO model could account for the systematic shifts of a series of lanthanide dimers observed for Bands I and II. The interaction between the monomeric MOs increases with decreasing size of central metal, resulting in a spectral blue-shift and red-shift corresponding to the HOMO→SOMO (Band I) and SOMO→LUMO transitions (Band II). The spectral changes on going from the neutral form to the reduced or oxidized forms were also successfully explained using the MO models: since the Nc−OEP distance decreases in the order of $[M(Nc)(OEP)]^-$ > $[M(Nc)(OEP)]$ > $[M(Nc)(OEP)]^+$, the bonding or antibonding interactions of the constituent monomeric MOs become larger in the same order. The DFT calculations agree well with the conceptual model presented in this paper and succeeded in reproducing the experimental trends (i.e., the shift of the absorption band with ionic size of the rare-earth metal). This simple intuitive MO model was applied for the interpretation of the electronic absorption and MCD spectra of the OEP−Nc−OEP triple-decker systems ($M(Nc)(OEP)_2$, M = Eu, Nd), and succeeded in reasonably explaining the spectral shift with the size of the rare-earth metal and dispersion type Faraday *A*−term MCD curves. This study allows us to highlight the importance of bonding or antibonding MO interactions and the usefulness of MCD spectroscopy for understanding the electronic structures of heteroleptic sandwich species of porphyrinoids. The present MO model can afford a valuable insight in designing advanced molecular devices.

Acknowledgment. This research was partially supported by the Ministry of Education, Science, Sports, and Culture, Japan, a Grand-in-Aid for the COE project, Giant Molecules and Complex Systems, 2004, and by the Belgian Science Fund (FWO) and Concerted Action Scheme (GOA).

IC0502325